

STATISTICAL TOLERANCE TRANSFER FOR COMPLEX SHEET METAL PART FORMING

Wang Rui, Georg Thimm, and Ma Yongsheng
School of Mechanical & Aerospace Engineering,
Nanyang Technological University, Singapore
Email: MGEORG@ntu.edu.sg

ABSTRACT

Current process planning practice and theory for sheet metal part forming does not consider transfer of geometric tolerances (GD&T). To eliminate this shortcoming, GD&T tolerance transfer is implemented using a statistical model of machining errors and a Monte-Carlo simulation. Considered sources of errors comprise positioning errors of the part and bend lines, bending angles, and blanking. Typical sheet metal parts are studied.

KEYWORDS: Tolerance Transfer, Statistical Tolerancing, Sheet Metal Forming

1 INTRODUCTION

Process errors, design tolerance specifications, and production cost are closely interrelated. Precise knowledge of process errors and their accumulation with respect to design dimensions allows an optimal choice of processes (in particular the datums used in them) in terms of minimal machine and setup changes, as well as other cost related properties of processes. To no surprise, major efforts in calculating the -so called - tolerance transfer, were undertaken in the past and are ongoing for metal removal processes and assembly (Thimm, 2001; Hong, 2002; Desrochers, 2003; Thimm, 2004; Lin, 2005). However, this is not true for sheet metal part forming: only specific work was done with respect to sheet metal and does not comprise transfer of geometric tolerances (GD&T) (De Vin, 1996; De Vin 1998; Han, 2001; Aomura, 2002; Rico, 2003).

According to publications in this field, researchers feel that several issues need to be addressed:

- Angular errors for bending operations (erroneous estimations of spring-back) influence also the accuracy of size dimensions. In literature on tolerance transfer this issue is widely overlooked.
- Charting methods for tolerance transfer consider space only two dimensions.
- Only size dimensional tolerances (conventional plus/minus) are considered. De Vin stated that it is necessary to transfer size tolerances to geometric tolerances but no details were discussed (De Vin, 1998).
- Computer aided tolerancing has to be extended to operations other than bending. Operations such as punching, blanking, and deep-drawing are neglected.
- Statistical tolerancing is utilized only for tolerance analysis and synthesis of sheet metal assembly issues, not for sheet metal part forming (Singh, 2003).

In the aim of initiating a more detailed investigation, effects of process errors such as workpiece positioning errors, errors on the positions of bend lines, and errors on bend angles on the tolerances of the part are modelled and calculated.

As a generalisable and closed form for statistical tolerances seems to be not achievable, a Monte-Carlo simulation is used to determine actual error distributions. Even so the Monte-Carlo method is of limited use in practical applications, the authors feel that it is an important step in this investigation, as it will allow an objective evaluation of other methods (Landau, 2005). This is of particular importance in sheet metal forming due to rather complex interactions of various errors (certain errors can cancel each other).

The feasibility to calculate geometric tolerances is demonstrated for two geometric dimensions in two example parts. Furthermore, a calculation of part tolerances provides an insight into the accumulation of geometric tolerances.

2 TOLERANCE TRANSFER IN SHEET METAL FORMING

2.1 MACHINING ERRORS IN BENDING AND PUNCHING

Before the examination of the two example parts in sections 2.2 and 2.4 can take place, process errors have to be discussed.

The prevailing part errors chosen for the examples in bending and punching processes are listed in table 1. All errors ΔE are considered to be independent statistical variables with centred normal distributions (the Δ labelling it as statistical variable). The notation δE designates a sample or *observed error* in the distribution ΔE . Errors are understood in the following as distributions (symmetric and free of systematic errors in order to simplify the notation). This means, that depending on the tolerance model (e.g. worst case or statistical) chosen, the “+” operator, as well as products, are to be interpreted accordingly.

Error	Symbol	Standard Deviation σ
Blanking error	ΔB	0.015mm
Positioning error	ΔP	0.015mm
Thickness error	ΔT	0.01mm
Error in length during bending	ΔL_b	0.01mm
Angular error in position of bends	$\Delta \gamma_b$	
Angular bending error	$\Delta \alpha$	0.1°
Error in length during punching	ΔL_p	0.01mm
Angular error in position of punched features	$\Delta \gamma_p$	

Table 1: Errors and their distribution in sheet metal forming

The blanking error ΔB is the distribution of the distance between the ideal and the actual outline of a sheet metal blank. For the same batch of metal blanks, this error is expected to follow the same distribution.

Positioning errors ΔP are the distances between individual, idealised datums and the corresponding point on the workpiece and cause an inaccurate workpiece setting. Figure 1 illustrates the errors for the position of a bend line (the line where the punch touches the part first). The position of the workpiece with respect to the datums a , b , and c (solid triangles indicate the operational datums) is affected by the observed errors $\delta P_a, \delta P_b, \delta P_c \in \Delta P$, resulting into the tolerance zone for the bend line ideally located at the dashed line. Depending on the positions of these datums and their relative errors, the actual bend line may be shifted, tilted, or both.

The error ΔT for the thickness of the sheet is assumed to affect a given blank uniformly. In other words, the thickness of a blank may deviate from the nominal value, but features everywhere the same thickness.

Let \mathbf{a} and \mathbf{b} be the 2-point datum (compare figure 1. Then, if the distance between the datums a and b is approximatively L , the workpiece is angularly displaced by angle β with:

$$\beta = \arctan \frac{\delta P_b - \delta P_a}{L} \quad (1)$$

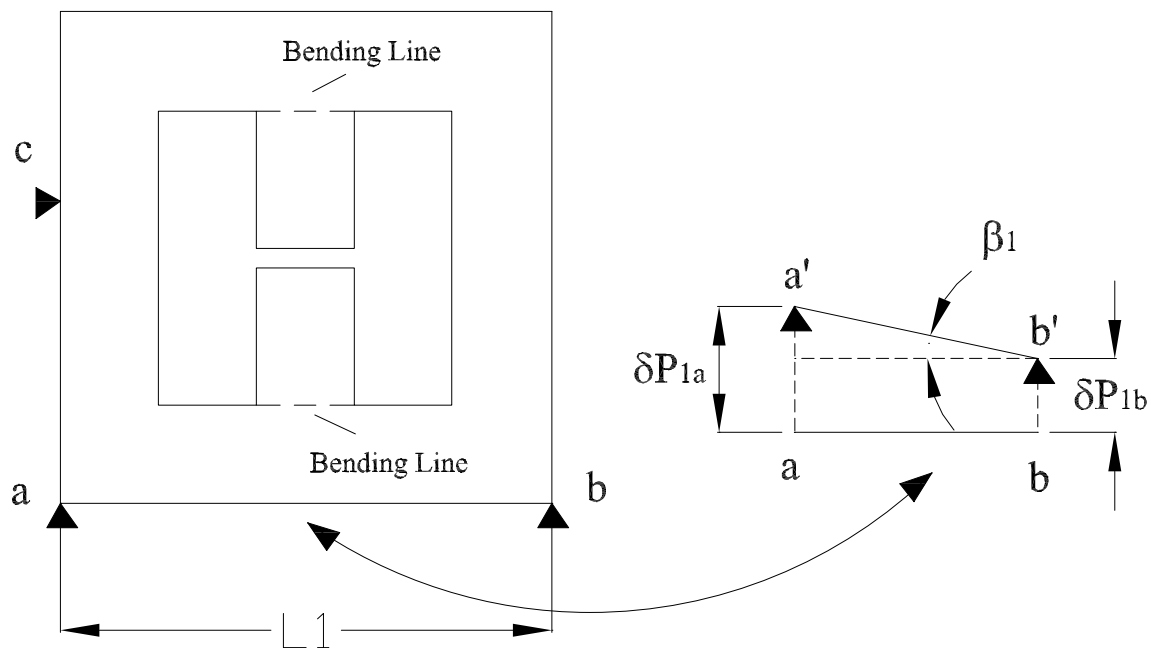


Figure 1: Positioning errors of operation 1

Furthermore, the bend line is linearly displaced by the average δP_a and δP_b if the bend line is parallel to the line defined by the 2-point datum or by the value of δP_c if the two lines are perpendicular.

Errors $\Delta L_b, \Delta \gamma_b, \Delta L_p,$ and $\Delta \gamma_p,$ for positions of bend lines and punched features are caused by:

- The inaccuracy of the machine tool setup. This comprises, for example, the inaccuracy of the punch position relative to the die. For one batch of workpieces bent on the same machine tool, the distribution of this inaccuracy can be considered as invariable.
- The inaccuracy of the forming process. Again, many factors are involved: the geometrical inaccuracy of the press, the alignment between the punch and the die, the deformation of the

processing system under external forces, vibrations, and thermal deformations (Wang, 1991).

- The difference between the real and estimated ideal lengths due to stretching of the workpiece.

As typical values of $\Delta\gamma_b$ and $\Delta\gamma_p$ are unknown to the authors and in order to simplify the mathematical notation, they are neglected in the following. The reader may, though, add whatever value she chooses to the β_i occurring in the formulae.

The angular error $\Delta\alpha$ of a bend is mainly caused by an inaccurate prediction of spring-back. It has a direct influence on geometrical tolerances. For the same batch of sheet metal, this distribution is constant and independent from the bending sequence. For example, if two surfaces are linked by a sequence of parallel bend lines, the angular error between these surfaces is the accumulation of the corresponding observed angular errors $\delta\alpha \square \Delta\alpha$.

Sheet metal is usually toleranced at a $\pm 2\%$ to $\pm 5\%$ variation in thickness. For 2mm of nominal sheet thickness and a $\pm 2\%$ tolerance region corresponds approximately to 0.01mm variance given in table 1 for a 6σ statistical tolerance.

The error ΔD of a hole in a punching process is typically caused by a dimensional error of the punch or the deflection between punch and die. This error is assumed not to change the centre of a hole (as in contrast to ΔL_p).

2.2 COMBINED SIZE AND PARALLELISM TOLERANCE

This section aims at demonstrating that sheet metal forming errors as listed in table 1 can cause both, dimensional as well as angular part errors. This is done using the part shown in figure 2. Focus is put on the dimension specified for surfaces $A2X$ and $A9Z$, which is a combination of size dimension L_4 with parallelism tolerance T_I . More precisely, this dimension specifies that all points of surface $A9Z$ must be within a distance in the range of $[L_4, L_4+T_I]$ to $A7Z$.

Figure 3 illustrates the forming process starting with a cut-to-size blank and the accumulation of sheet metal forming errors. Setups 1 to 4 depict the bending operations (starting with the bend between surfaces $A7Z$ and $A2X$). Operational datums are highlighted by solid triangles. No effort is made to choose datums such that the accumulation of process errors is avoided.

In general, an error E with respect to a dimension is the sum of the supposed independent dimensional and angular process errors, that is E_d and E_g . The independence of the two elements is in accordance with best practices and discussed in more detail in (Thimm, 2006). Then, for the example part in figure 2, the error E is with respect to dimension $A7Z$ - $A9Z$. In detail: $E(A7Z, A9Z) = E_d(A7Z, A9Z) + E_g(A7Z, A9Z)$.

Figure 3 illustrates the forming process starting with a cut-to-size blank and the accumulation of sheet metal forming errors. Setups 1 to 4 depict the bending operations (starting with the bend between surfaces $A7Z$ and $A9Z$). Operational datums are highlighted by solid triangles. No effort is made to choose datums such that the accumulation of process errors is avoided.

Figure 3 shows that the processes contributing to the tolerance stack for design dimension $A7Z$ - $A9Z$ are:

1. The distance between the blank surfaces $S1X0$ and $S4X0$ is affected by error:

$$E_d(S1X0, S4X0) = \delta B$$

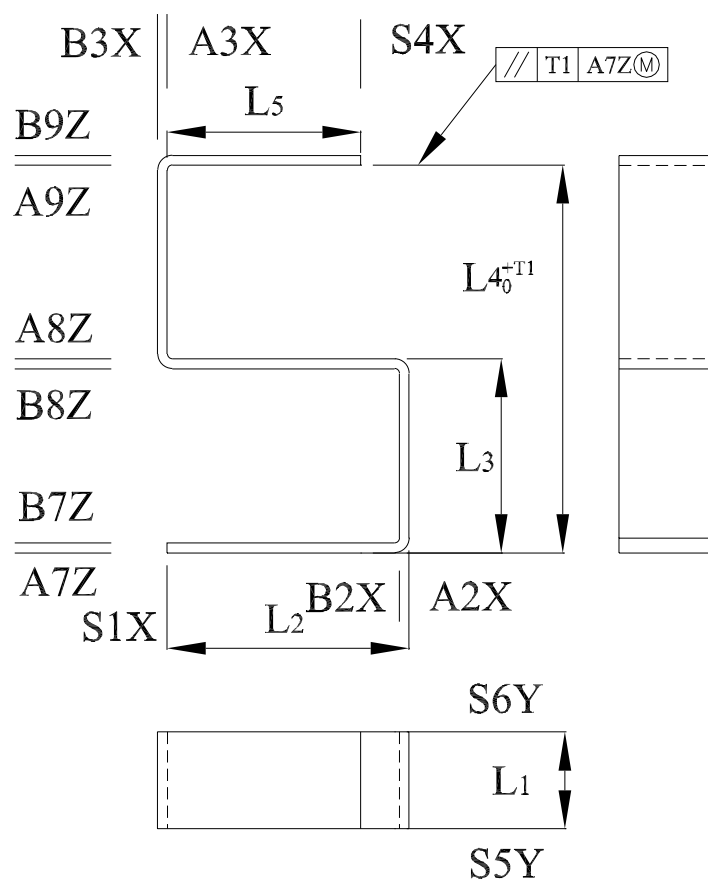


Figure 2: Engineering drawing of the example part

2. Bending operation 1 forms the surfaces¹ $A7Z0$, $B7Z0$, $A2X0$, $B2X0$, $A8Z0$, $B8Z0$, $A3X0$, $B3X0$, $A9Z0$, $B9Z0$, and $S4X1$:

$$E_d(S1X0, B2X0) = \delta L_{b1} + (\delta P_{1b} - \delta P_{1a}) + \frac{1}{2}(\delta P_{1b} + \delta P_{1a})$$

$$E_d(A7Z0, S4X1) = \delta B + \delta L_{b1} + (\delta P_{1b} - \delta P_{1a}) + \frac{1}{2}(\delta P_{1b} + \delta P_{1a}) + \delta T$$

3. Operation 2 creates the surfaces $A8Z1$ and $B8Z1$ and prepares the pre-forming surfaces $A3X1$, $B3X1$, $A9Z1$, $B9Z1$, and $S4X2$:

$$E_d(A7Z0, A8Z1) = \delta L_{b2} + (\delta P_{2b} - \delta P_{2a}) + \frac{1}{2}(\delta P_{2b} + \delta P_{2a}) + \delta T$$

$$E_d(B2X0, S4X2) = \delta B + \sum_{i=1}^2 (\delta P_{ib} - \delta P_{ia}) + \frac{1}{2}(\delta P_{ib} + \delta P_{ia}) + \delta L_{bi}$$

¹ Note that $L_i \tan(\beta_i) = \delta P_{ib} - \delta P_{ia}$

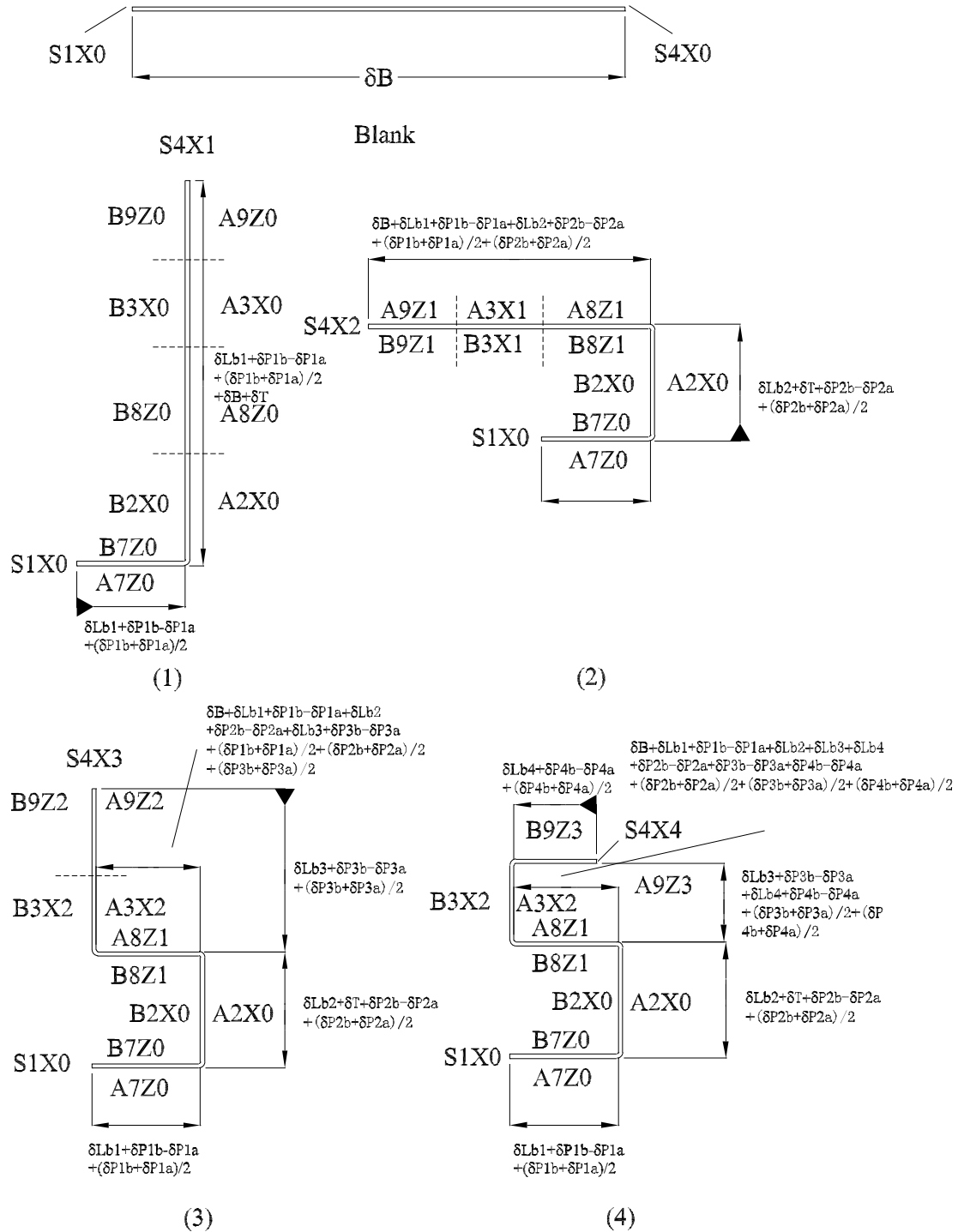


Figure 3: A detailed analysis of tolerance stacks for the bending sequence

4. Operation 3 forms surfaces $A3X2$, $B3X2$, $A9Z2$, $B9Z2$, and $S4X3$:

$$E_d(S4X3, A8Z1) = \delta L_{b3} + (\delta P_{3b} - \delta P_{3a}) + \frac{1}{2}(\delta P_{3b} + \delta P_{3a})$$

$$E_d(B2X0, A9Z2) = \delta B + \sum_{i=1}^3 (\delta P_{ib} - \delta P_{ia} + \frac{1}{2}(\delta P_{ib} + \delta P_{ia})) + \delta L_{bi}$$

5. Operation 4 creates surfaces *A9Z3*, *B9Z3*, and *S4X4*:

$$E_d(S4X4, A3X2) = \delta L_{b4} + (\delta P_{4b} - \delta P_{4a}) + \frac{1}{2}(\delta P_{4b} + \delta P_{4a})$$

$$E_d(A8Z1, A9Z3) = \sum_{i=3}^4 (\delta P_{ib} - \delta P_{ia} + \frac{1}{2}(\delta P_{ib} + \delta P_{ia})) + \delta L_{bi}$$

The error caused by dimensional process errors between *A7Z0* and *A9Z3* for the final part consequently is $E_d = E_d(A9Z3, A8Z1) + E_d(A7Z0, A8Z1)$.

However, angular errors of the bends (the estimation of spring-backs) also contribute to the dimensional error between *A7Z0* and *A9Z3*. For example as shown in figure 4, the position of the second bend line with respect to *A7Z* is affected by the observable angular error $\delta\alpha_i \square \Delta\alpha$ and the distance between the first and second bend line. The corresponding error E_{g1} can be written as: $E_{g1} = L_3[\cos(\delta\alpha_1) - 1]$. The calculation can be carried on as illustrated in figure 4 (all $\delta\alpha_i \square \Delta\alpha$):

$$E_{g2} = (L_2 - t) \sin(\delta\alpha_1 + \delta\alpha_2)$$

$$E_{g3} = (L_4 - L_2)[\cos(\delta\alpha_3 - \delta\alpha_2 - \delta\alpha_1) - 1]$$

$$E_{g4} = L_5 \sin(\delta\alpha_4 + \delta\alpha_3 - \delta\alpha_2 - \delta\alpha_1)$$

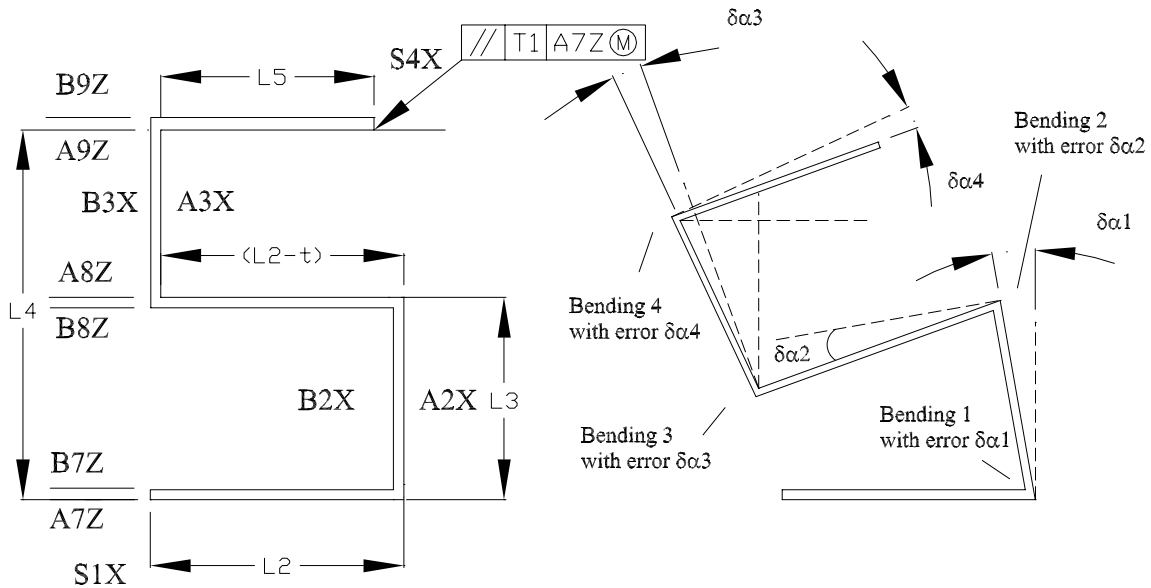


Figure 4: The tolerance analysis of the angular errors

Therefore, the error between *A7Z0* and *A9Z3* for the final part is:

$$E(A9Z3, A8Z1) = \sum_{i=2}^4 (\delta P_{ib} - \delta P_{ia} + \frac{1}{2}(\delta P_{ib} + \delta P_{ia})) + \delta L_{bi} + \delta T + L_3[\cos(\delta\alpha_1) - 1] \\ + (L_2 - t)\sin(\delta\alpha_1 + \delta\alpha_2) + (L_4 - L_3)[\cos(\delta\alpha_3 - \delta\alpha_2 - \delta\alpha_1) - 1] + L_5 \sin(\delta\alpha_4 + \delta\alpha_3 - \delta\alpha_2 - \delta\alpha_1)$$

Setting $L_1=20\text{mm}$, $L_2=50\text{mm}$, $L_3=L_5=40\text{mm}$, $L_4=80\text{mm}$, and $t=2\text{mm}$ as well as using the errors given in table 1 permits to determine the distribution of the error $E(A9Z3, A8Z1)$ by the means of a Monte Carlo simulation over ten thousand samples. The resulting histogram of the distribution of $E(A9Z3, A8Z1)$ (calculated using intervals with a width of 0.01mm) is show

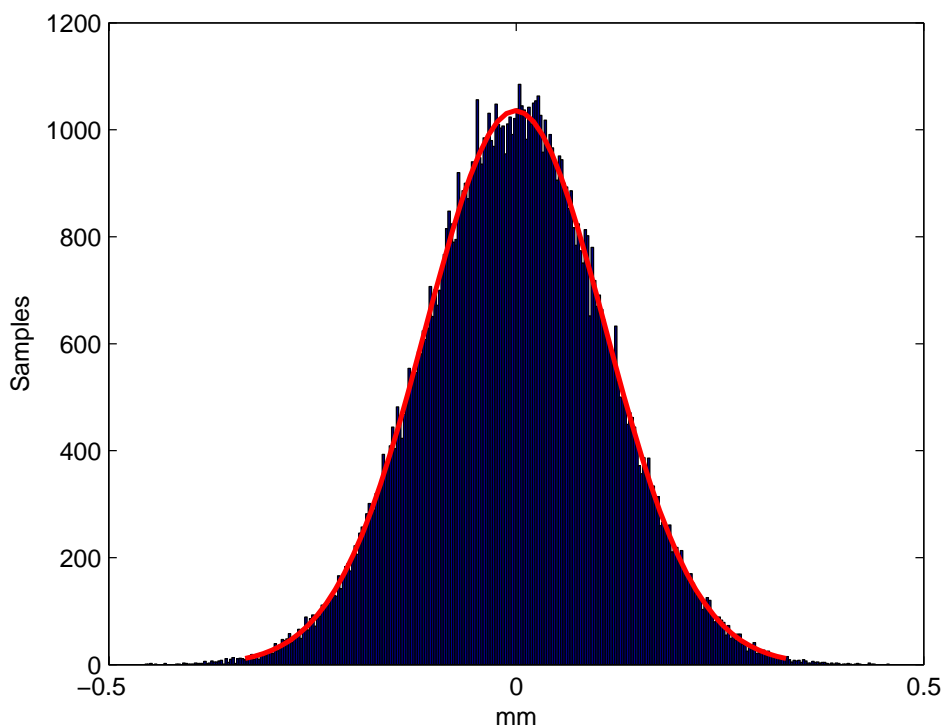


Figure 5: Histogram of $E(A9Z3, A8Z1)$

The figure includes both the histogram of the data and a normal distribution with the sample mean and standard deviation as the sample distribution of $E(A9Z3, A8Z1)$, showing its similarity to a normal distribution. Both, the sample mean and median are statistically zero. The standard deviation of $E(A9Z3, A8Z1)$ is approximately 0.1106mm with a mean of 0.00001mm.

In the aim of better understanding the influence of the components of this error on its total, its partial differentials with respect to each statistical variable were calculated. In short, this allowed to conclude that:

- The dimensional errors ΔL_b , ΔT , and ΔP change the part dimensions in the range of their own distribution: $\frac{\partial E}{\partial(\delta L_{bi})}, \frac{\partial E}{\partial(\delta T)}, \frac{\partial E}{\partial(\delta P_{i(a,b)})} = const.$

- The error committed during the estimation of a spring-back is in the order of the part's size dimensions:

$$\frac{\partial E}{\partial(\delta\alpha_1)} \approx -L_3, \frac{\partial E}{\partial(\delta\alpha_2)} \approx L_2 - t, \text{ and } \frac{\partial E}{\partial(\delta\alpha_3)}, \frac{\partial E}{\partial(\delta\alpha_4)} \approx L_5$$

Consequently, the error on the spring-back likely contributes more to the size dimensional errors of the final part than the dimensional error themselves.

For comparison, tolerance intervals of $\pm 3\sigma$ for the machining were used to calculate worst case errors. This results in: $-0.8937 \leq E(A9Z3, A8Z1) \leq 0.8916$. This interval is, as it can be expected, too large as compared to the statistical result.

2.3 PARALLELISM TOLERANCE

In contrast to the last section, only the parallelism between the two surfaces is considered (that is the absolute distance is ignored). This changes the terms describing the accumulated error: the error in length ΔL_{bi} and the terms for linear displacements of the workpiece relative to the datums (that is the terms $\frac{1}{2}(\delta P_{ib} + \delta P_{ia})$) and the part have to be disregarded. The error with respect to the parallelism between *A7Z0* and *A9Z3* becomes:

$$E(A9Z3, A8Z1) = \sum_{i=2}^4 (\delta P_{ib} - \delta P_{ia}) + L_3 [\cos(\delta\alpha_1) - 1] + (L_2 - t) \sin(\delta\alpha_1 + \delta\alpha_2) \\ + (L_4 - L_3) [\cos(\delta\alpha_3 - \delta\alpha_2 - \delta\alpha_1) - 1] + L_5 \sin(\delta\alpha_4 + \delta\alpha_3 - \delta\alpha_2 - \delta\alpha_1)$$

For the same experimental setup, the distribution of $E(A9Z3, A8Z1)$ has the same shape with a statistically zero mean and a slightly smaller standard deviation of 0.1070mm.

2.4 POSITION TOLERANCE

The two holes *H18XZ* and *H19XZ* in the part shown in figure 6 are positioned relative to each other. Their axes are constrained by a position tolerance relative to datum **A** (the surface *A15Z* at the bottom of the part). A coordinate system is set up as shown in the lower right image of figure 6 and all size design dimensions are labelled with L_i ($i=1, 2, 3\dots$).

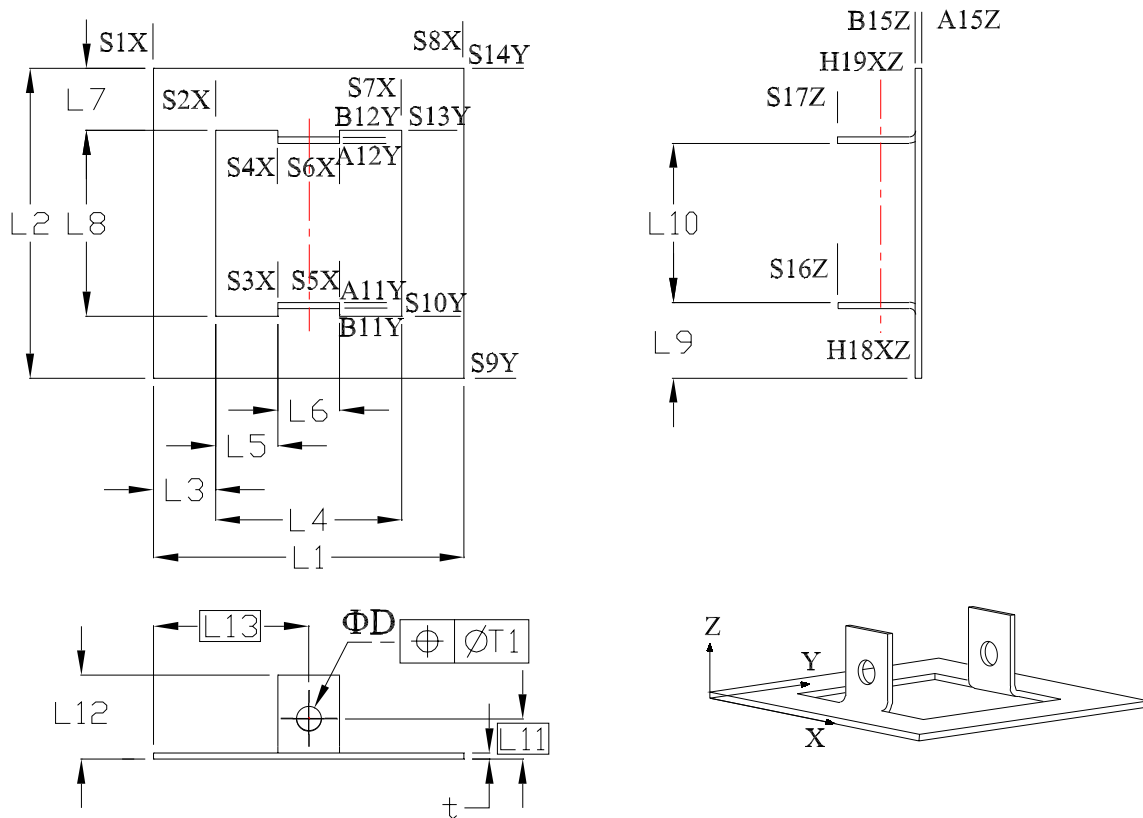


Figure 6: Labelling and dimensions of the example part

An operation sequence (blanking, punching, and two bending operations) is illustrated in figures 7 to 9. For this sequence, the observed error E for the position of the holes $H18XZ$ and $H19XZ$ is calculated. The position errors can be calculated with L_{13} and β_i ($i=1, 2, 3, \dots$).

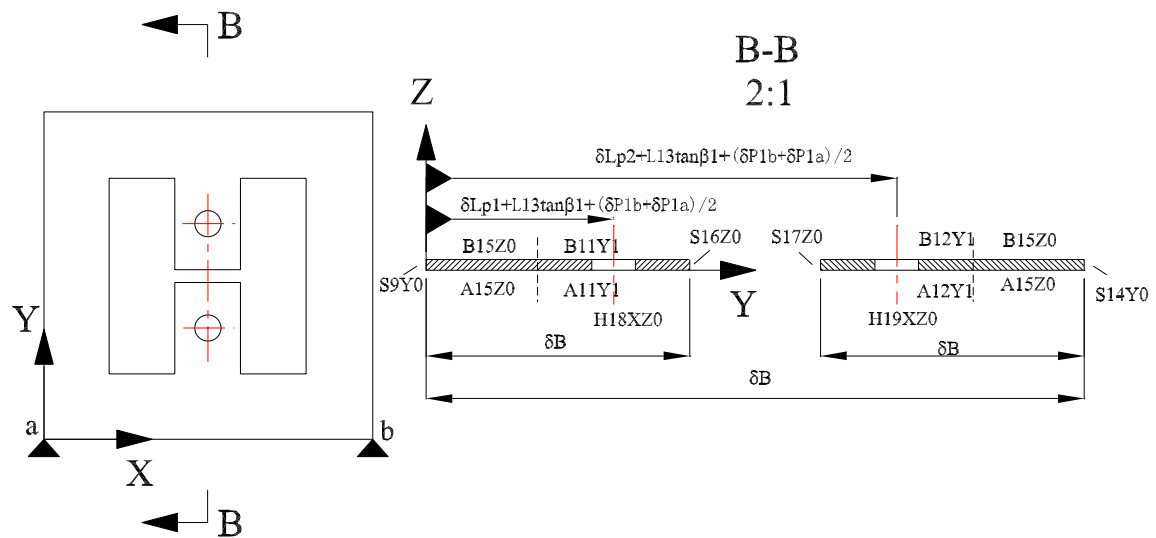


Figure 7: Operation 1: punching the holes $H18XZ0$ and $H19XZ0$

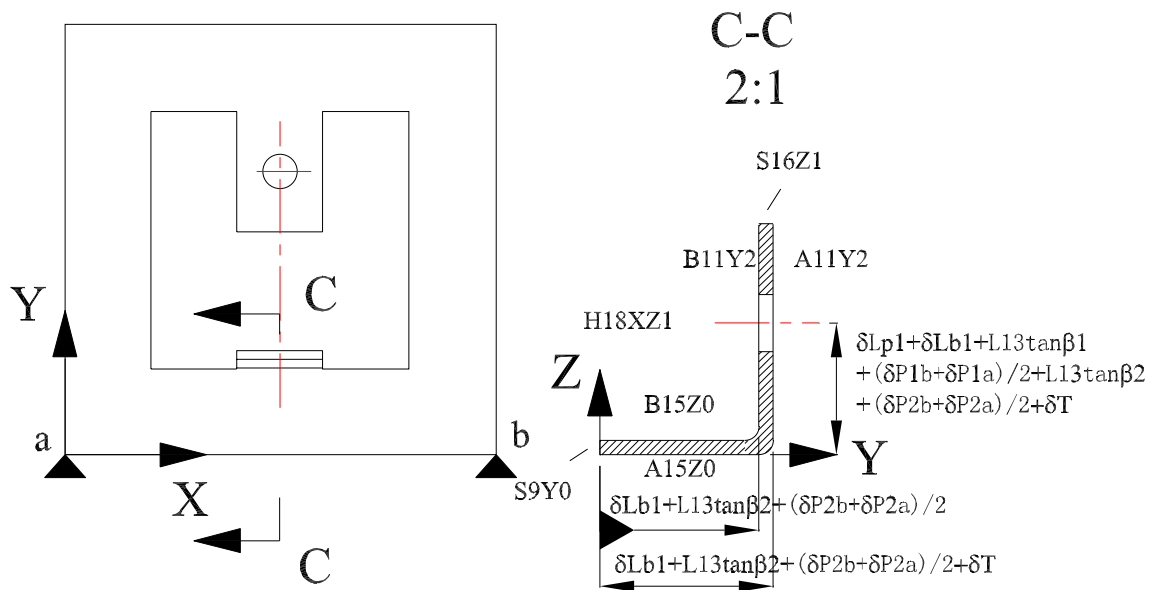


Figure 8: Operation 2: bending

If the 2-point datum is placed on surfaces $S9Y0$ or $S14Y0$, the tolerances of the process are:

1. The blanking operation forms the side surfaces and the surfaces forming the H-shaped hole with the error ΔB . This error affects all distances between any pair of surfaces, but does contribute at most once to any tolerance chain.
2. Operation 1 punches $H18XZ0$ and $H19XZ0$.

$$E_d(S9Y0, H18XZ0) = \delta L_{p1} + L_{13} \tan(\beta_1) + \frac{1}{2}(\delta P_{1b} + \delta P_{1a})$$

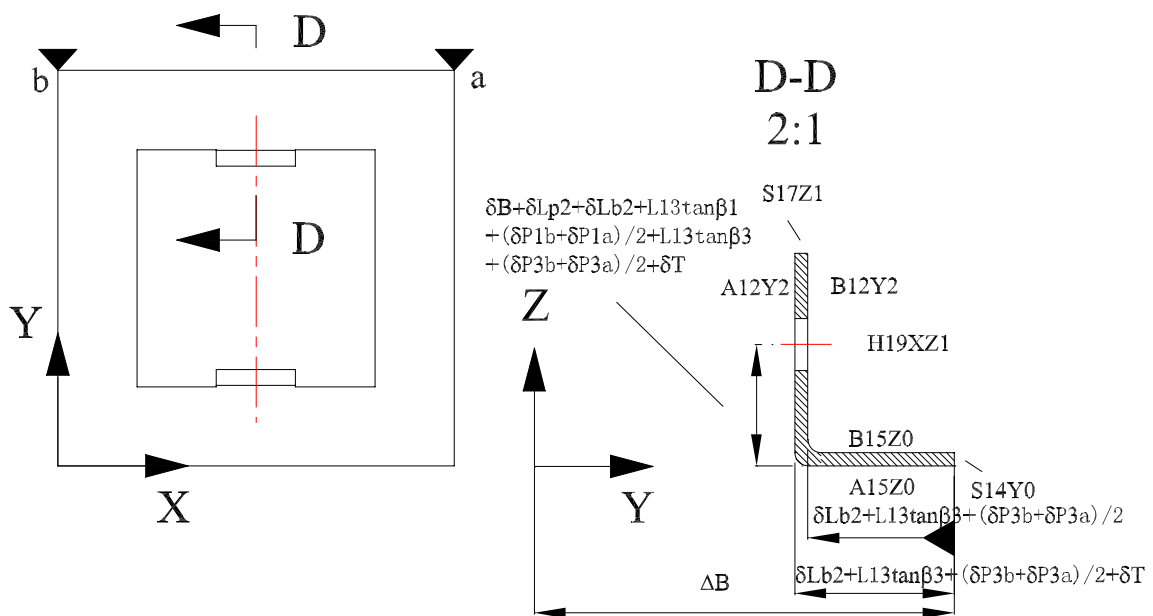


Figure 9: Operation 3: bending

$$E_d(S9Y0, H19XZ0) = \delta L_{p2} + L_{13} \tan(\beta_1) + \frac{1}{2}(\delta P_{1b} + \delta P_{1a})$$

$$E_d(S14Y0, H19XZ0) = \delta B + \delta L_{p2} + L_{13} \tan(\beta_1) + \frac{1}{2}(\delta P_{1b} + \delta P_{1a})$$

with β_1 are given in equation (1), that is $L_{13} \tan(\beta_1) = \frac{L_{13}}{L_1}(\delta P_{ib} - \delta P_{ia})$.

3. Operation 2 (Bending 1) creates *A11Y2*, *B11Y2*, *S16Z1*, and *H18XZ1*.

$$E_d(A15Z0, H18XZ1) = \delta L_{p1} + \delta L_{b1} + L_{13} \tan(\beta_1) + L_{13} \tan(\beta_2) + \delta T \\ + \frac{1}{2}(\delta P_{1b} + \delta P_{1a}) + \frac{1}{2}(\delta P_{2b} + \delta P_{2a})$$

4. Operation 3 (Bending 2): the features *A12Y2*, *B12Y2*, *S17Z1*, and *H19XZ1* are formed.

$$E_d(A15Z0, H19XZ1) = \delta B + \delta L_{p2} + \delta L_{b2} + L_{13} \tan(\beta_1) + L_{13} \tan(\beta_3) + \delta T \\ + \frac{1}{2}(\delta P_{1b} + \delta P_{1a}) + \frac{1}{2}(\delta P_{3b} + \delta P_{3a})$$

However, the error between the axes of the holes *H18XZ* and *H19XZ* is also affected by angular process errors, as illustrated in figure 10.

According to ISO specification 1101 and 5458, the position tolerance zone is limited by a cylinder of diameter T_I , with reference to the surfaces *A15Z* and *S1X*. The errors in the direction of the x- and z-axis must be compared with T_I to assert that the holes are within the tolerance zone. Therefore, the extreme locations of the four points **A**, **B**, **C** and **D** in the direction of three axes have to be compared with the part's specification.

The displacements of these points, which are caused by size dimensional and angular process errors with respect to the orientation of the three axe, are given in tables 2 and 3, respectively (table 3 assumes that the bend lines are perfectly parallel to *S9Y0*). The sums of corresponding entries in these two tables are the maximal displacement of each point in the respective orientations.

In figure 11, point **O** is the nominal position of the centre of the hole, which is decided by two basic size dimension L_{11} and L_{13} . The actual centre line of the two holes is controlled by the circular tolerance zone with a specified diameter T_I . **A**, **B**, **C** or **D** locates in the tolerance zone.

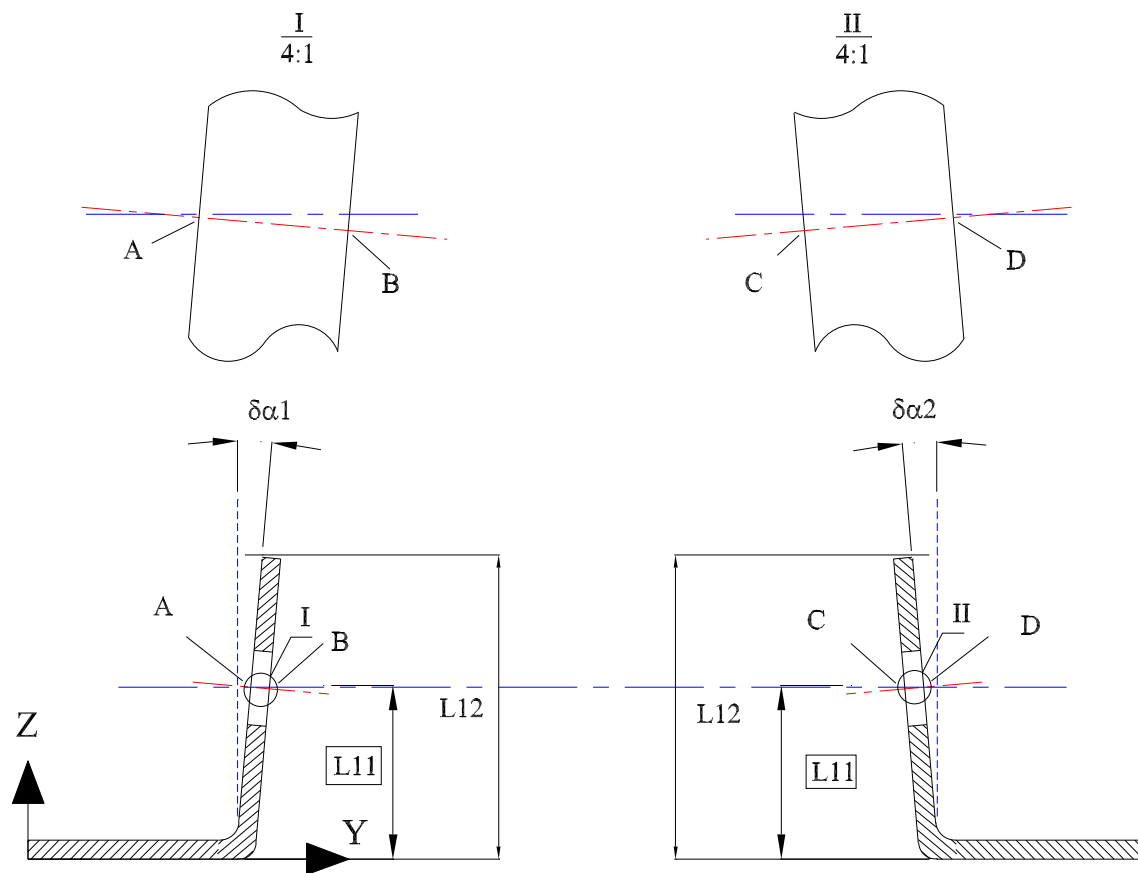


Figure 10: Analysis of the angular error

Point	x	z
A, B	$\delta L_{p1} + \delta P_{1c}$	$\delta L_{p1} + \delta L_{b1} + L_{13} \tan(\beta_1) + L_{13} \tan(\beta_2) + \frac{1}{2}(\delta P_{1a} + \delta P_{1b})$ $+ \frac{1}{2}(\delta P_{2a} + \delta P_{2b}) + \delta T$
C, D	$\delta L_{p1} + \delta P_{1c}$	$\delta L_{p2} + \delta L_{b2} + L_{13} \tan(\beta_1) + L_{13} \tan(\beta_3) + \frac{1}{2}(\delta P_{1a} + \delta P_{1b})$ $+ \frac{1}{2}(\delta P_{3a} + \delta P_{3b}) + \delta T + \delta B$

Table 2: Displacements of points by dimensional errors with respect to the three axes

Point	x	z
A	0	$L_{11} (\cos(\delta\alpha_1) - 1)$
B	0	$(L_{11} + t)(\cos(\delta\alpha_1) - 1)$
C	0	$(L_{11} + t)(\cos(\delta\alpha_2) - 1)$
D	0	$L_{11} (\cos(\delta\alpha_2) - 1)$

Table 3: Displacements of points by angular process errors with respect to the three axes

According to ISO 5458, the axis of the hole must be located within the tolerance zone. Be r_A , r_B , r_C , and r_D the Euclidean distances between **O** and the four points **A**, **B**, **C** or **D**, then the part is within specification if:

$$P_d := 2 \cdot \max\{r_A, r_B, r_C, r_D\} \leq T_1$$

The distances r_A , r_B , r_C , and r_D are the Euclidean distances in the x-z plane of the respective points, that is the sums of the coordinates in tables 2 and 3, to point (L_{13}, L_{11}) .

The distribution of P_d was estimated using a Monte-Carlo simulation over ten thousand random samples $L_I=50\text{mm}$, $L_{II}=15\text{mm}$, $L_{13}=25\text{mm}$, $t=2\text{mm}$, and the errors as given in table1).

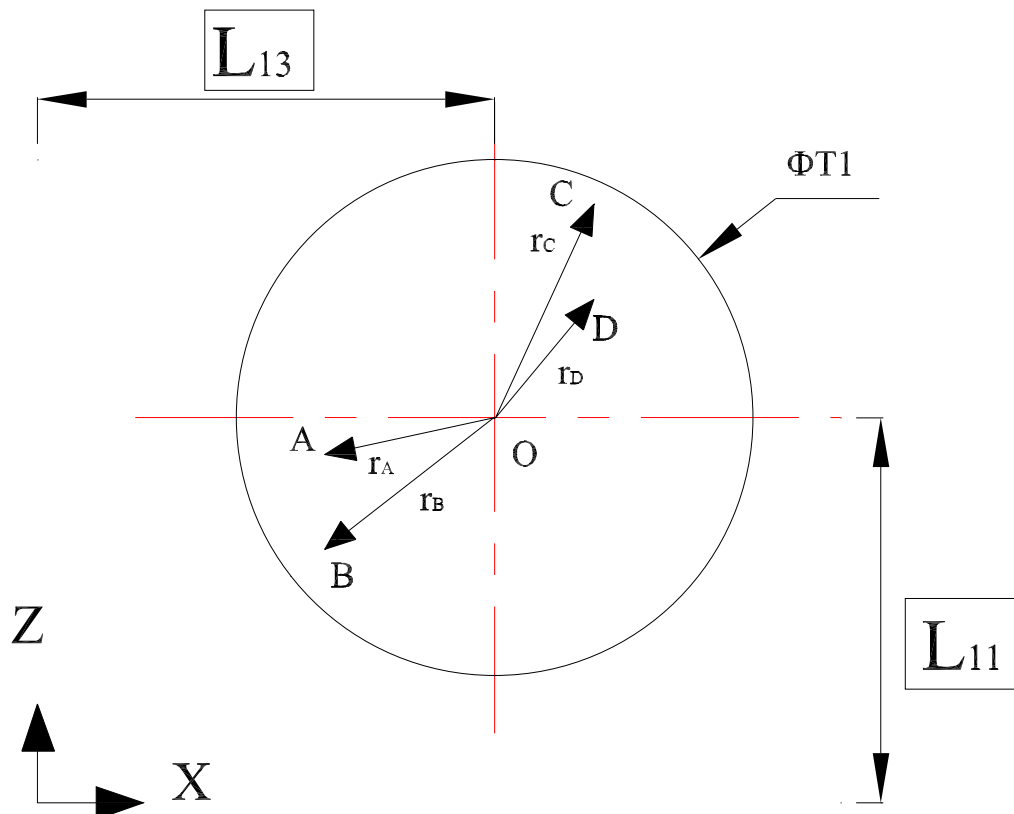
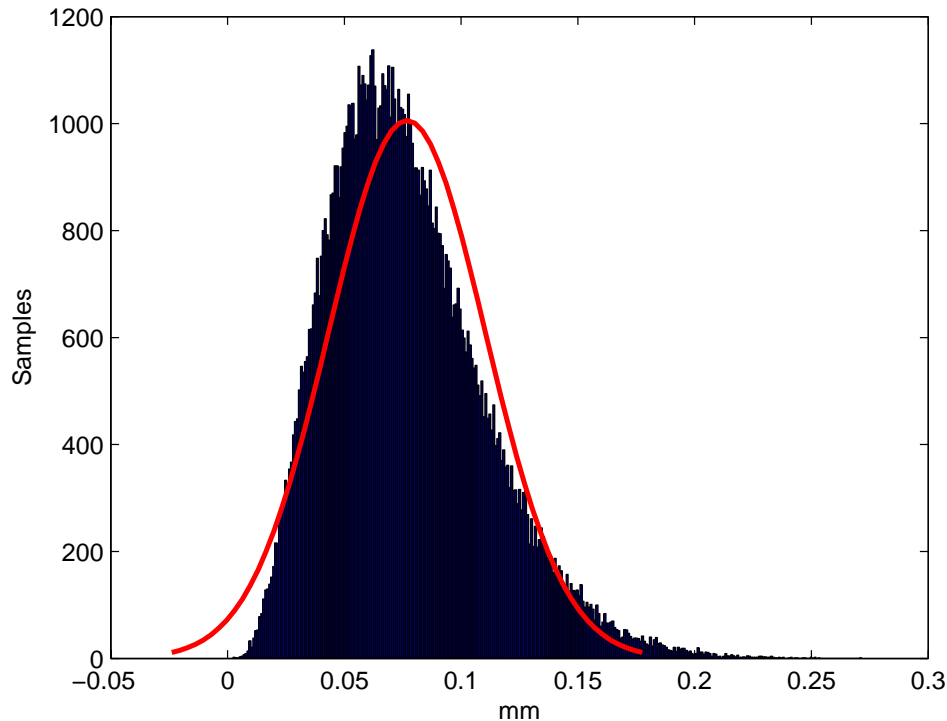


Figure 11: Positional Tolerance Zone

Figure 12 shows both a frequency histogram of P_d based on 0.01 wide intervals and the envelope of a normal distribution using the sample median value (0.076840mm) and standard deviation (0.033599mm) of the data for comparison. Obviously the distribution of P_d is not a normal distribution, nor has a near-zero mean.

A worst case model with tolerance intervals of $\pm 3\sigma$, results into an estimation of P_d with $0 \leq P_d \leq 0.64806$ mm. Obviously, the upper value of the interval much bigger than the values obtained by the statistical approach, whereas the mean is close to the statistical value.

Figure 12: Histogram of P_d

3 CONCLUSION

The paper demonstrates that geometric tolerance transfers from process tolerances to geometric dimensions of the design can be calculated. The proposed method relies statistical tolerancing using a Monte-Carlo simulation in combination of closed forms for the deviations of the part's shape based on geometrical tolerances of machining processes in a sheet metal forming sequence. Major sources of machining errors are considered, including angular errors caused by spring-back.

A comparison of the error distributions with values obtained from a worst-case analysis for 6- σ confidence intervals showed, that - as it is also observable for prismatic or rotational parts - the latter often grossly overestimates the errors for the part. However, this problem is more pronounced in sheet-metal parts, as tolerance chains tend to include more processes and approaches like direct machining (Boothroyd, 2002; Thimm, 2004) are more difficult to apply. A further remarkable difference to other types of machining processes is that, even though process tolerances are centred, this may not be true for the errors of the final part.

REFERENCES

- Aomura S., Koguchi A. Optimized bending sequences of sheet metal bending by robot. *Robotics and Computer Integrated Manufacturing*, 18; 1; 2002 p.29-39.
- Boothroyd G., Dewhurst P. and Knight W. *Product design for manufacture and assembly*. Marcel Dekker, 2nd edition, 2002.
- De Vin L.J. , Streppel A.H., and Kals H.J.J. The accuracy aspect in set-up determination for sheet bending. *International Journal of Advanced Manufacturing Technology*, 11; 1996, p. 179-185.

- De Vin L.J., Streppel A.H. Tolerance reasoning and set-up planning for brakeforming. *International Journal of Advanced Manufacturing Technology*, 14; 1998, p.336-342.
- Desrochers A. A CAD/CAM representation model applied to tolerance transfer methods. *Journal of Mechanical Design*, 125; 1; 2003, p.14-22.
- Hong Y.S., Chang T. C. A comprehensive review of tolerancing research. *International Journal of Production Research*, 40; 11; 2002, p. 2425-2459.
- ISO 1101. Geometrical Product Specification (GPS) - Geometrical tolerancing – Tolerances of form, orientation, location and run-out, 2002.
- ISO 5458. Geometrical Product Specifications (GPS) - Geometrical tolerancing – Positional tolerancing, 1998.
- Landau D.P. A guide to Monte Carlo simulations in statistical physics, Cambridge University Press, 2005.
- Rico J. C., Gonzalez J.M., Mateos S., et al. Automatic determination of bending sequences for sheet metal parts with parallel bends. *International Journal of Production Research*, 41; 14; 2003, p.3273-3299.
- Singh S.K., Jain S.C., and Jain P.K. Tolerance analysis of mechanical assemblies using Monte Carlo simulation. *International Journal of Industrial Engineering - Theory Applications and Practice*, 10; 2; 2003, p.188-196.
- Thimm G. and Lin J. Redimensioning parts for manufacturability: A design rewriting system. *The International Journal of Advanced Manufacturing Technology*, 26; 4; 2005, p.399-404.
- Thimm G., Britton G.A., and Cheong F.S. Controlling Tolerance Stacks for Efficient Manufacturing. *The International Journal of Advanced Manufacturing Technology*, 18; 1; 2001, p.44-48.
- Thimm G., Britton G.A., and Cheong F.S. How CNC process plans constrain designs of rotational parts: a rigorous approach. *Computer-Aided Design & Applications*, 1; 1-4; 2004, p.359-366.
- Thimm G., Britton G.A., and Fok S.C. A graph theoretic approach linking design and process planning, part 1: design to process planning. *The International Journal of Advanced Manufacturing Technology*, 24; 3-4; 2004, p.261-271.
- Thimm G., Britton G.A., and Whybrew K. Optimal process plans for manufacturing and tolerance charting. *Proceedings of the Institution of Mechanical Engineers. Part B, Journal of Engineering Manufacture*, 215; B8; 2001, p.1099-1105.
- Thimm G., Wang R., and Ma Y.S. Tolerance transfer in sheet metal forming. *International Journal of Production Research*, 2006. accepted.
- Wang H.P. and Li J.K. *Computer-Aided Process Planning*. Elsevier Science Publishers, Amsterdam, Netherlands, 1991.